involved in may be central to the pathogenesis of ALS and FTLD. Intriguingly, under diverse stress conditions, TDP-43 and FUS proteins are reported to localize to stress granules (SGs), cytoplasmic messenger ribonucleoproteins (mRNPs) in which non-translating mRNA, many translation initiation components and RNA-binding proteins accumulate (Colombrita *et al.* 2009; Liu-Yesucevitz *et al.* 2010; Dewey *et al.* 2011; McDonald *et al.* 2011; Meyerowitz *et al.* 2011). These stresses inducing SGs limit protein synthesis, mostly via inhibition of translation initiation (Anderson and Kedersha 2009). mRNA translation and stability in SGs may play important roles in determining cell fate during stress. Mild or intermediate stress causes the recovery of translation and the synthesis of proteins essential for adaptation followed by cell survival. However, prolonged or severe stress promotes cell death, mostly via inducing apoptosis. In fact, SGs harbor several apoptosis regulatory factors and affect cell survival rates following exposure to stress (Buchan and Parker 2009). Thus, the cellular response to stress involves regulation of mRNA translation, for example, the synthesis of pro-survival or pro-apoptotic proteins. However, the exact nature of this mechanism in affected brain regions from patients with ALS or FTLD remains unresolved. Therefore, identifying pathological alterations of mRNA metabolism occurring in these diseases will provide important insights into the pathogenesis of these diseases.

In this study, we examined the physiological roles of TDP-43 in the complex translational regulation mechanisms determining cell fate under conditions of oxidative stress. Under oxidative stress induced by sodium arsenite (ARS), which induces cells to assemble cytoplasmic stress granules (SGs), multimolecular aggregates of stalled translation preinitiation complexes that prevent the accumulation of misfolded proteins (Arimoto *et al.* 2008), we found that TDP-43 associated with stalled ribosomes, and appears to play an important role(s) in mRNA stability and cell survival.

Methods

Cell culture, transfection, plasmids, reagents, antibodies, Western blotting, immunocytochemistry, RNAi experiments, and quantitative assessment of cell death

Detailed procedures are described in the previous study (Higashi *et al.* 2010) and the Supplemental methods.

Polysome profile analysis by linear sucrose gradient fractionation

Polysome profile analysis was carried out as previously described (Kawai *et al.* 2004; Lu *et al.* 2009) with minor modifications. HeLa cells were grown in 10-cm dishes to about 80% confluence. After some treatments with ARS, cells were cultured in medium with 0.1 mg/mL cycloheximide (Sigma-Aldrich, St. Louis, MO, USA) at 37°C for 3 min for analysis of polyribosomes as previously described (Feng *et al.* 1997). Cells were washed twice with cold phosphate-buffered saline (PBS) containing 0.1 mg/mL cycloheximide, and then lysed in polysome lysis buffer containing 15 mM Tris-HCl, pH 8.0, 300 mM NaCl, 15 mM $MgCl_2$, 1% Triton X-100, 1 mg/mL heparin and 0.1 mg/mL cycloheximide on ice for 10 min. Lysates were centrifuged at 10 000 *g* for 10 min. For the RNase experiments, prior to ultracentrifugation, lysates were treated with 300 μg/mL RNase A at 30°C for 15 min as previously described (Ceman *et al.* 2003). For fractionation, a total of 1 mL of the supernatant obtained from three 10-cm dishes was loaded onto 10 mL of 10–50% sucrose gradients containing 15 mM Tris-HCl, pH 8.0, 300 mM NaCl, 5 mM $MgCl_2$, 0.5 mg/mL heparin, 0.1 mg/mL cycloheximide in Ultra-Clear Centrifuge Tubes (14 × 89 mm, Beckman, Palo Alto, CA, USA), and separated by ultracentrifugation with a SW41 rotor (Beckman) at 35 000 rpm at 4°C for 90 min. Each gradient was collected into 1-mL fractions from bottom with the ribosomal profile monitored by absorbance measurements at 260 nm (Atto, Tokyo, Japan). Equal volumes from each fraction were used for Western blotting.

Fluorescence *in situ* hybridization

Control or TDP-43-silenced SH-SY5Y cells were prepared in six-well plates as described in the Supplementary Methods section. After incubation with reagent, cells were rinsed with TBS, fixed with 4% paraformaldehyde for 10 min, permeabilized with 100% methanol for 10 min at −20°C, and then rehydrated for 1 h at 4°C with 70% ethanol. After incubation in 1 M Tris-HCl (pH 8.0) for 5 min at 22°C, cells were hybridized overnight at 37°C with 1 μg/mL Cy™3-oligo-dT(30) in hybridization buffer (1 mg/mL yeast tRNA, 0.005% bovine serum albumin , 10% dextran sulfate, 25% deionized formamide, 2 × SSC). After washing, sections were incubated for 3 h with anti-TDP-43 antibody at a 1 : 200 dilution in 0.1% Triton X-100 in 2 × SSC at 22°C. After further washing, sections were incubated for 2 h with Cy™2-conjugated secondary antibody (Jackson ImmunoResearch Lab, Inc., Baltimoer Pike, PO) at a 1 : 200 dilution in 0.1% Triton X-100 in 2 × SSC at 22°C. After incubating with 4′, 6-diamidino-2-phenylindole (DAPI) for 2 min, the cover slips were washed and mounted in mounting medium. Mean fluorescence intensity per cell in each siRNA-transfected cell was calculated from three independent experiments using Zeiss LSM ZEN 2010 software (Carl Zeis MicroImaging GmbH, Jena, Germany) according to the manufacturer's instructions.

Results

TDP-43 associates with stalled ribosomes under oxidative stress

To understand the physiological roles of TDP-43 in translational regulation, we conducted polysome profile analysis in HeLa cells treated with ARS. After treatment with cycloheximide to trap elongating ribosomes, HeLa cells were lysed with polysome lysis buffer containing Triton X-100 and heparin to extract membrane-bound polysomes and stabilize RNA (Gauthier and Ven Murthy 1987) and then fractionated on a 10–50% sucrose density gradient. Ultracentrifugation allowed separation of the ribosomal subunits and polysome profiles were then obtained by absorbance measurements at 260 nm during fraction collection.

The polysome profile under the steady-state condition, including peaks for the 40S and 60S ribosomal subunits, 80S

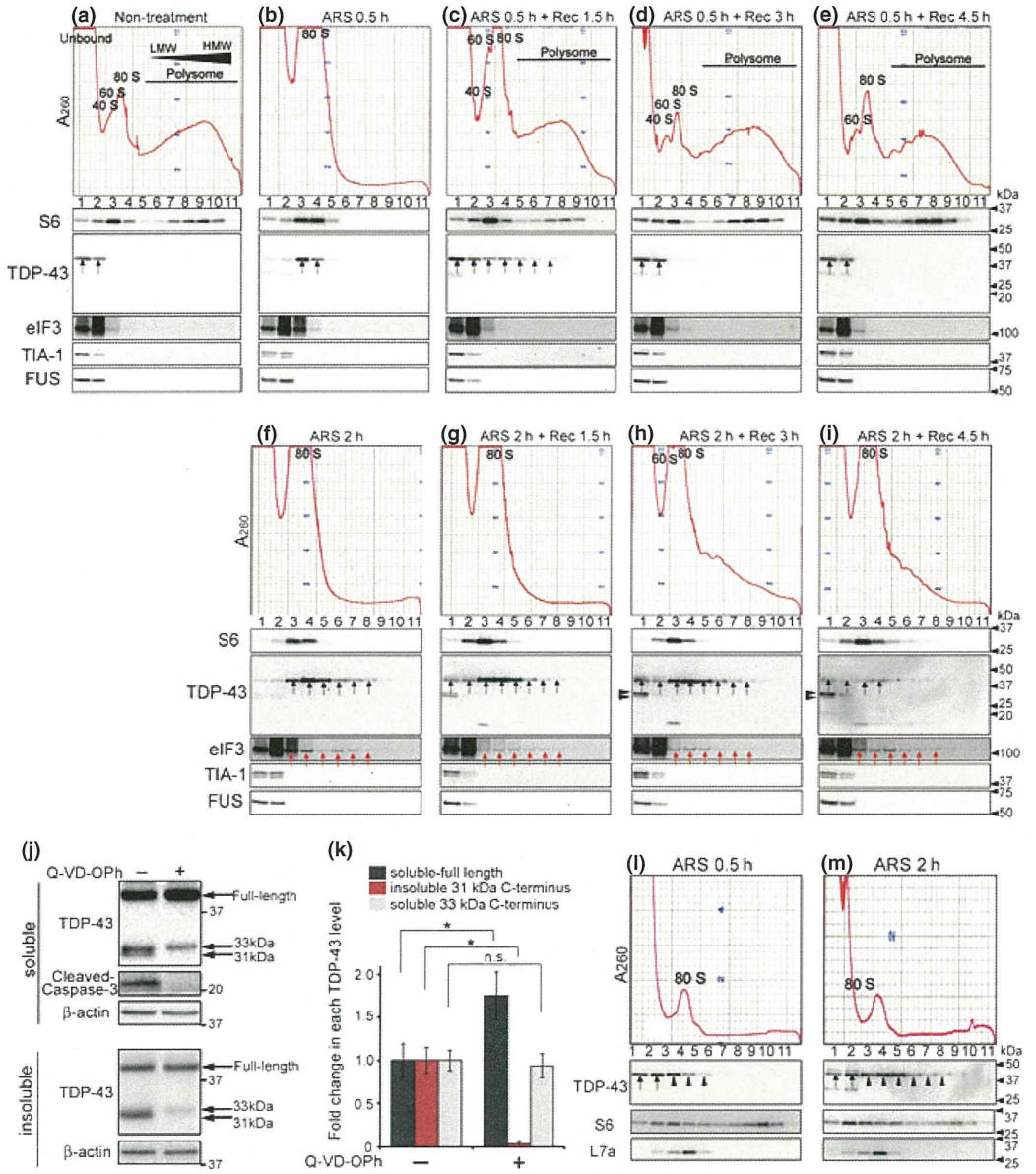

monosomes and actively translating polysomes, is indicated in Fig. 1a. The 40S ribosomal protein S6 co-fractionated with the major monosome (Fig. 1a fractions 2–4) or polysome (Fig. 1a fractions 6–10). Under this normal condition, TDP-43 was found in fractions of lower density devoid of ribosomes (Fig. 1a fractions 1 and 2). Other SG-associated RNA-binding proteins, namely, TIA-1, FUS (Fig. 1a), HuR, and G3BP1 (data not shown), also remained in the non-ribosomal fraction, while eIF3 was partially fractionated to the 40S ribosomal fraction as previously reported (Kedersha *et al.* 2002) (Fig. 1a fraction 3). Previous studies have reported that TDP-43 is incorporated into SGs in response to several stress stimuli (Colombrita *et al.* 2009; Liu-Yesucevitz *et al.* 2010; Dewey *et al.* 2011; McDonald *et al.* 2011; Meyerowitz *et al.* 2011). To characterize the molecular properties of TDP-43 under the stress condition, we treated cells with ARS, which induces oxidative stress followed by formation of SGs. ARS treatment for 0.5 h induced dissociation of polysomes and a shift of S6 to the high monosomal peak, suggesting that the monosomal peak includes some SG components, such as stalled ribosomes and mRNAs (Fig. 1b fractions 3 and 4). In fact, this treatment induced formation of SGs in which TIA-1 and S6 were co-localized (Fig. 2b and g). In these treated cells, TDP-43 and some eIF3 were fractionated to the monosomal fractions from the non-ribosomal fractions (Fig. 1b fractions 3 and 4), while FUS, TIA-1, HuR, and G3BP1 remained in fractions at the top of the gradients (Fig. 1b and data not shown). Thus, TDP-43 not only localized to SGs (Fig. 2g) but also was able to

Fig. 1 (a–i) The A_{260} absorbance profile for RNAs separated by sedimentation velocity through a 10–50% leaner sucrose gradient is shown in the top panel to indicate the sedimentation of 40S ribosomal subunits, 60S subunits, 80S monosomes, and polysomes. Fractions 1 and 2 represent non-ribosomal fractions, in which the expected peaks for tRNAs and other small RNAs obscured by the high absorbance are observed. Cell extracts obtained from untreated HeLa cells (a), and those treated with 0.5 mM sodium arsenite (ARS) for 0.5 h (b) or 2 h (f), or treated with 0.5 mM ARS for 0.5 h or 2 h and then allowed to recover in ARS-free media (denoted as Rec) for the indicated times (c–e, g–i) were layered on the top of the gradients; then, after ultracentrifugation, 1-mL fractions were collected. An equal volume of each fraction was subjected to immunoblot analysis with anti-S6 (small ribosomal subunits), anti-TAR DNA-binding protein 43 (TDP-43) (recognizing the carboxyl (C)-terminal region), anti-eIF3, anti-TIA-1, or anti-FUS antibody. Black arrows or arrowheads indicate the distribution of full-length or C-terminal (approximately 31 kDa and 33 kDa) TDP-43 in the gradient, respectively. Red arrows indicate the distribution of eIF3 to the heavy fraction. (j) HeLa cells were pre-treated with or without 10 μM Q-VD-OPh (general caspase inhibitor) for 1 h, and then treated with 0.5 mM ARS with or without 10 μM Q-VD-OPh for 2 h followed by recovery in ARS-free media with or without 10 μM Q-VD-OPh for 4.5 h. After cells were harvested with cold 1% Triton X-100 lysis buffer, soluble and insoluble fractions were analyzed by immunoblotting as indicated. (k) The relative levels of soluble full-length TDP-43 (black), insoluble 31 kDa (red) and soluble 33 kDa (gray) C-terminal TDP-43 were quantified by densitometry and then normalized to the β-actin level. Data are presented as fold changes in the amount of Q-VD-OPh-treated cells compared with that of non-treated cells (mean ± SD, $n = 3$). *$p < 0.05$, n.s. = not significant (paired Student's *t*-test). (l, m) Soluble extracts from HeLa cells treated with 0.5 mM ARS for 0.5 h (l) or 2 h (m) were subjected to RNase A treatment (300 μg/mL) prior to ultracentrifugation, and then fractionated on a sucrose gradient. The collected fractions were analyzed by immunoblotting as indicated. Arrows indicate RNA-bound TDP-43 that was shifted to the top of the gradient by RNA digestion. Arrowheads indicate RNase treatment-resistant TDP-43 in the heavy fractions.

associate with stalled ribosomes (Fig. 1b) in response to stress stimuli. When polysomes were partially recovered 1.5 h after the stress was removed, most TDP-43 dissociated from ribosomal fractions and migrated to non-ribosomal fractions (Fig. 1c fractions 1 and 2), while some TDP-43 was fractionated into heavy fractions together with re-forming polysomes (Fig. 1c fractions 5–7). With longer recovery in ARS-free media, TDP-43 in the ribosomal fractions completely disappeared and migrated into the non-ribosomal fractions (Fig. 1d and e), suggesting that TDP-43 might be temporarily associated with ribosomes.

Long-term exposure of ARS delays disassociation of TDP-43 from stalled ribosomes during recovery and causes an increase in the amount of caspase-independent carboxyl-terminal TDP-43

We next investigated the molecular properties of TDP-43 in cells with long-term exposure to ARS. ARS treatment for 1 h induced migration of TDP-43 to the heavy fractions 5 and 6, in addition to fractions 3 and 4 (Figure S1a, arrows). In cells that had recovered from this treatment, dissociation of SGs and re-formation of polysomes were delayed, as shown in Figure S1b–d, while a small amount of S6 migrated to fractions 5–8, suggesting that polysomes were partially recovered. In these cells, a significant amount of TDP-43 remained in fractions 3–6 until at least 3 h after the stress was removed (Figure S1c). However, finally, most TDP-43 shifted to non-ribosomal fractions 1 and 2 while the monosomal peak remained in fractions 3 and 4 (Figure S1d). In addition, two bands for carboxyl (C)-terminal TDP-43 (approximately, 31 kDa and 33 kDa) were observed in the non-ribosomal fraction (Figure S1c, d fraction 1 arrowheads). As recovery time increased, only the amount of 33 kDa C-terminal TDP-43 increased.

ARS treatment for 2 h induced a shift of TDP-43 to the heavier fractions (Fig. 1f fractions 5–8). The shift of S6 to the heavy fractions was negligible even 4.5 h after the stress was removed (Fig. 1i), suggesting that long-term stress irreversibly inhibited global reformation of polysomes. In addition, an increase in the amount of the 33 kDa C-terminal TDP-43 was more prominent in 2-h-treated cells than in 1-h-treated ones (Fig. 1i arrowheads). Notably, eIF3 was also shifted to the heavy fractions in 2-h-treated cells (Fig. 1f–i red arrows).

We next investigated whether the C-terminal TDP-43 fragments shown in Fig. 1i were generated by activated caspases, which is reported to cleave the C-terminus of TDP-43 (Zhang *et al.* 2007). In fact, cleavage of caspase-3 was induced in cells that had recovered from 2 h of ARS treatment (Fig. 1j). In these cells, 33 kDa and 31 kDa C-terminal TDP-43 were mainly detected in Triton X-100-soluble and -insoluble extracts, respectively (Fig. 1j). Treatment with the general caspase inhibitor Q-VD-OPh caused the 31 kDa C-terminal TDP-43 to completely disappear, but the level of the 33 kDa species was unaffected by this treatment (Fig. 1j and k). In addition, caspase inhibition increased the amount of soluble full-length TDP-43 (Fig. 1j and k).

TDP-43 associates with stalled ribosomes by binding to mRNA

To investigate whether the ARS-induced TDP-43-ribosome association is RNA dependent, we treated lysates with RNase A to remove mRNA associated with ribosomes, without disturbing individual ribosomes (Nelson *et al.* 1992; Ceman *et al.* 2003). RNA digestion induced a shift of approximately 50% (48.5 ± 1.7%, mean ± SD, $n = 3$) of TDP-43 from the monosomal peak (Fig. 1l arrowheads) to the non-ribosomal fractions 1 and 2 (Fig. 1l arrows) in 0.5-h-treated cells, suggesting that a significant amount of TDP-43 is associated with stalled ribosomes by binding to mRNAs. However, in contrast, in 2-h-treated cells, only approximately 22% (21.6 ± 4.7%, mean ± SD, $n = 3$) of TDP-43 was shifted

to the non-ribosomal fraction by RNA digestion (Fig. 1m arrows). In particular, TDP-43 in heavy fractions 5–8 remained following RNA digestion (Fig. 1m arrowheads). In contrast, these alterations of TDP-43 were not observed in the control experiment (data not shown). Thus, the association of TDP-43 with stalled ribosomes by binding to mRNA was disturbed in cells exposed to severe stress. We also investigated whether the distribution of S6 and 60S ribosomal protein L7a would be altered by RNA digestion. RNA digestion induced a redistribution of S6 to the heavy fractions while L7a protein, which is known to be not included in SGs, remained in fractions 3–5 (Fig. 2l and m), suggesting that RNA is required for assembly of small ribosomal subunits into fractions 3 and 4.

TDP-43 is excluded from SGs after long-term exposure to ARS

We investigated the stress duration-dependent change in the subcellular localization of TDP-43, S6 and TIA-1 in cells treated with ARS for different periods of time. Both TDP-43 and S6 localized to TIA-1-positive SGs following 0.5 h of ARS treatment (Fig. 2b and g), and then redistributed to nuclear and cytoplasmic localizations similar to those in the normal condition when SG disassembly occurred following the removal of the stress (Fig. 2c and h). However, TDP-43 was excluded from TIA-1-positive SGs by 2 h of ARS treatment (Fig. 2i), and then localized to the cytoplasm with fine granular morphology in cells that had recovered (Fig. 2j inset). Thus, TDP-43 appears to be able to shuttle in and out of SGs according to the stress condition. Importantly, while polysome profile analysis demonstrated that the inhibition of reformation of polysomes was retained in 2-h ARS-treated cells, even after the removal of the stress (Fig. 1f–i), immunocytochemistry revealed that SG disassembly occurred in this condition (Fig. 2e and j), suggesting that the disturbance of translational initiation after long-term stress was not caused by abnormal continuous accumulation of SGs.

TDP-43-specific siRNA silencing reduces the monosomal peak after long-term exposure to ARS

We next investigated the effect of TDP-43 depletion on the polysome profile using siRNA. Our siRNA experiment induced ~90% silencing of TDP-43 expression in both Triton X-100-soluble and -insoluble extracts (data not shown). Under the non-stress condition, actively translating polysomes normally appeared in both control siRNA- and TDP-43 siRNA-transfected cells (data not shown). A monosomal peak was found in both transfected cells when they were treated with ARS for 0.5 h (data not shown), and the reformation of polysomes were also initiated in both cell types 3 h after the stress was removed (Fig. 2k). However, when cells were treated with ARS for 2 h, the size of the monosomal peak dramatically decreased during the recovery period in TDP-43-silenced cells compared with control cells (Fig. 2l). Western blot analysis revealed that the distribution of S6 was not altered in either group of cells (Fig. 2l). In addition, we quantified the amount of β-actin protein in cell extracts before ultracentrifugation on a sucrose gradient to demonstrate that the equal amounts of cells were subjected to the UV recordings in either group of cells. In fact, the amounts of β-actin protein in cell extracts were equal in both control siRNA- and TDP-43 siRNA-transfected cells (Fig. 2m). The amounts of S6 and other SG-associated RNA-binding proteins, such as TIA-1 and FUS, were also unaltered in both cells (Fig. 2m). Thus, in cells with long-term exposure to ARS, TDP-43-silencing caused a decrease in the amount of non-translating mRNA, measured based on the absorbance at 260 nm.

N-terminal region and RRM domains are responsible for ARS-induced disulfide bond formation and increased insolubility of TDP-43, respectively, while the C-terminus of TDP-43 has a tendency to become insoluble regardless of the stress

It has been suggested that the components of SGs are enriched in insoluble fractions (Cuesta *et al.* 2000; Kim *et al.* 2005). To assess the change in detergent-solubility of TDP-43 according to stress conditions, we quantified the amount of TDP-43 in the Triton X-100-soluble and insoluble fractions in cells treated with ARS for different periods of time. Soluble full-length TDP-43 levels were decreased by ARS treatment, while insoluble levels were increased; these levels were almost reversed to the steady-state amounts by the removal of the stress when ARS incubation time was 0.5 h, but not when it was more than 1 h (Fig. 3a and b). As shown in a previous report (Cohen *et al.* 2011), 120-kDa disulfide cross-linked TDP-43 can be detected by Western blotting under non-reducing conditions without 2-mercaptoethanol after ARS treatment (Fig. 3a). Disulfide cross-linked TDP-43 levels were also reversed to the steady-state amounts by the removal of the stress when ARS incubation time was 0.5 h, but not when it was more than 1 h (Fig. 3a and c). Thus, such biochemical alterations of TDP-43 were temporary in cells with exposure to short-term stress, but became irreversible in those exposed to long-term stress. In addition, 31-kDa caspase-dependent C-terminal TDP-43 levels in the insoluble fractions increased following the removal of the stress only when ARS incubation time was 2 h, in cells in which caspase-3 was activated (Fig. 3a and d). We investigated the change in insolubility of other SG-associated proteins. The solubility of S6 was barely altered by ARS treatment. In contrast, the solubilities of TIA-1, FUS and HuR were altered; the amount of TIA-1 in the insoluble fraction increased following ARS treatment, consistent with the previous study, in which TIA-1 has been reported to be aggregated in SGs (Gilks *et al.* 2004). However, the amounts of FUS and HuR in the insoluble fraction decreased (Fig. 3a).

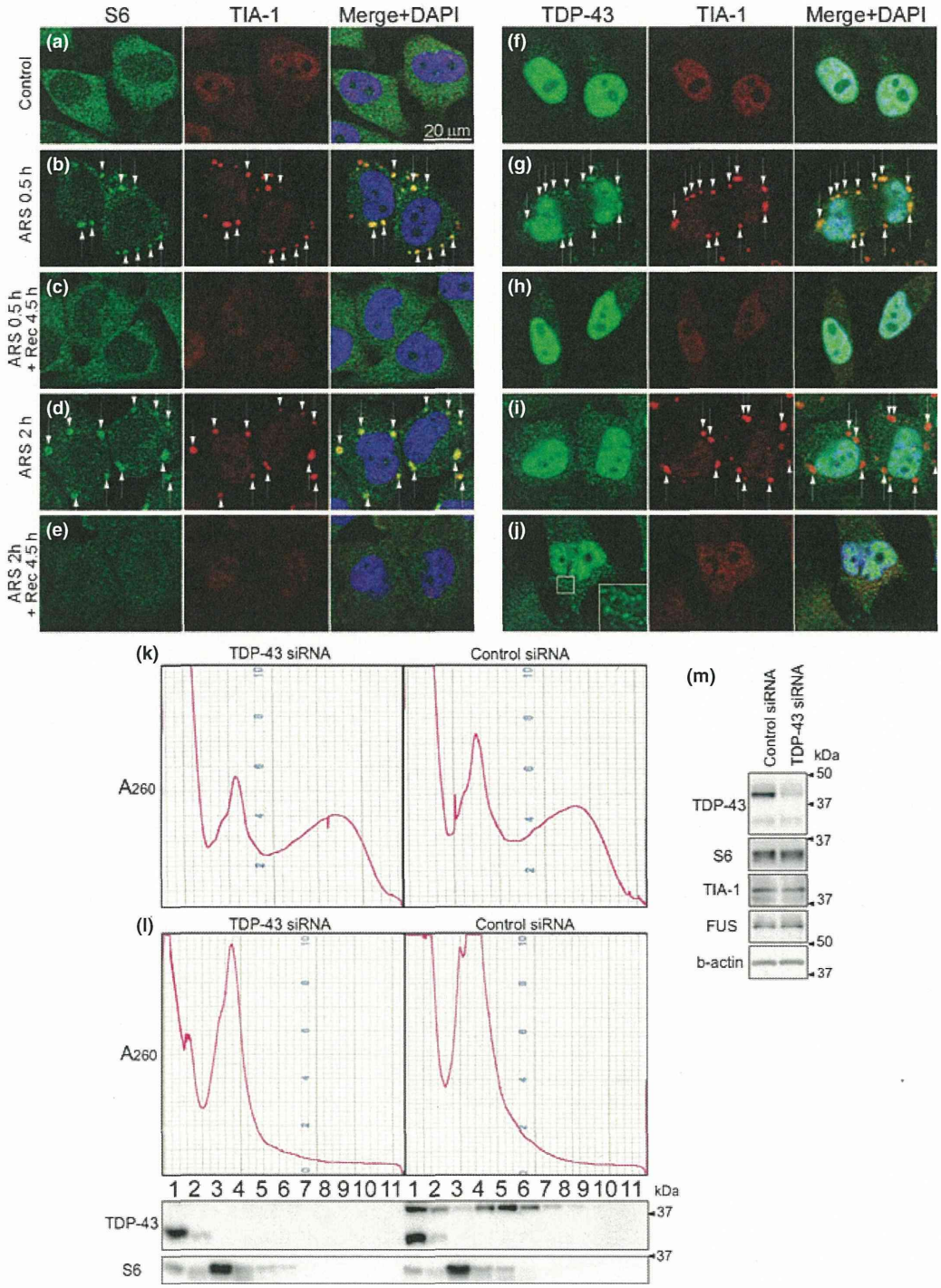

Fig. 2 (a–j) HeLa cells were untreated (Control) or treated with 0.5 mM sodium arsenite (ARS) with or without subsequent recovery in ARS-free media for the indicated times, and then analyzed by immunocytochemistry as indicated. Arrows in (b, d, g, and i) indicate stress granules (SGs). The inset in (j) highlights TAR DNA-binding protein 43 (TDP-43)-positive cytoplasmic granular compartments. 4′, 6-diamidino-2-phenylindole (DAPI). (k, l) Control siRNA or TDP-43 siRNA-transfected cells were treated with 0.5 mM ARS for 0.5 h (k) or 2 h (l) followed by recovery in ARS-free media for 3 h. The collected fractions in panel (l) were analyzed by immunoblotting as indicated. (m) Extracts harvested from control siRNA or TDP-43 siRNA-transfected cell before ultracentrifugation on the sucrose gradient used in panel (l) were analyzed by immunoblotting as indicated.

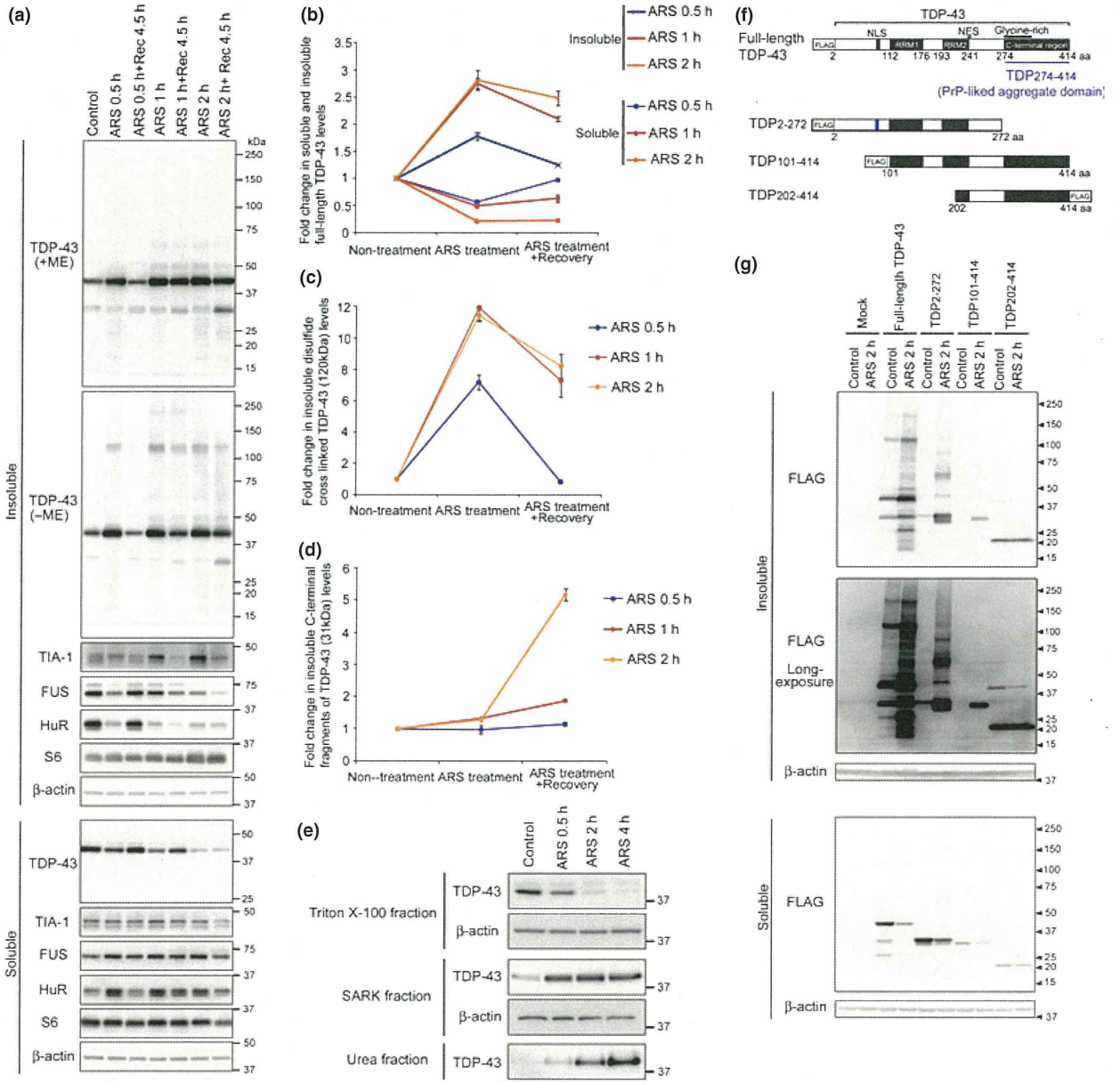

Fig. 3 (a–g) Soluble and insoluble fractions extracted from untreated HeLa cells (Control) or HeLa cells treated with 0.5 mM sodium arsenite (ARS) with or without subsequent recovery in ARS-free media as indicated with cold 1% Triton X-100 lysis buffer (see Methods) were analyzed by immunoblotting as indicated. (b–d) Levels of full-length (b), 120 kDa disulfide cross-linked (c) or 33 kDa C-terminal TAR DNA-binding protein 43 (TDP-43) (d) in soluble and insoluble fractions were quantified by densitometry and then normalized to the β-actin level. Data are presented as fold change compared with non-treated controls (mean ± SD, $n = 3$). (e) The sequential extraction of untreated HeLa cells (Control) or HeLa cells treated with 0.5 mM ARS for indicated times with Triton X-100, sarkosyl (SARK) and urea lysis buffer (See Methods) were analyzed by immunoblotting as indicated. (f) Schematic representations of the protein domain architecture of full-length or deletion mutants of TDP-43 are shown. The amino acid (aa) residues of TDP-43, the nuclear localization sequence (NLS), the nuclear export sequence (NES), the glycine-rich region, and the prion protein (PrP)-like aggregate domain ($TDP_{274-414}$) are indicated. (g) Soluble and insoluble fractions extracted from untreated HeLa cells (Control) or HeLa cells treated with 0.5 mM ARS for 2 h were analyzed by immunoblotting as indicated.

We sequentially extracted cells treated with ARS for different periods of time using Triton X-100, SARK and urea lysis buffer (See Methods). In cells treated with ARS for 0.5 h, most of the TDP-43 in the Triton X-100-insoluble pellet was solubilized in SARK buffer (Fig. 3e). However, in cells treated with ARS for 2 or 4 h, SARK-insoluble TDP-

43, reminiscent of pathogenic aggregated TDP-43 (Arai *et al.* 2006), was detected in the urea fraction (Fig. 3e).

We used cells over-expressing deletion mutants of TDP-43 with a FLAG tag at the N- or C-terminus, as shown in Fig. 3f, to investigate which region of TDP-43 is responsible for such increased insolubility or disulfide bond formation. Full-length TDP-43 or TDP-43 without the C-terminal region ($TDP_{2\text{-}272}$) showed increased insolubility and disulfide bond formation following ARS-induced stress. In contrast, TDP-43 without the N-terminal region ($TDP_{101\text{-}414}$) did not form disulfide bonds, but showed an increase in protein insolubility (Fig. 3g). When TDP-43 without both the N-terminal region and RRM domains ($TDP_{202\text{-}414}$), the domain structure of which is similar to that of C-terminal TDP-43, was expressed, neither disulfide bond formation nor increased protein insolubility occurred following ARS-induced stress. Thus, the N-terminal region and RRM domains are responsible for ARS-induced disulfide bond formation and the increased insolubility of TDP-43, respectively. Intriguingly, the amount of $TDP_{202\text{-}414}$ in the insoluble fraction was increased in cells without ARS treatment, while both $TDP_{2\text{-}272}$ and $TDP_{101\text{-}414}$ were barely detected in the insoluble fraction from cells without ARS treatment, suggesting that the C-terminus of TDP-43 has a tendency to become insoluble regardless of the stress.

Phosphorylated TDP-43 co-localizes with an ubiquitin-binding protein, p62

Previous reports have demonstrated that several stress stimuli induce phosphorylation of TDP-43 (Ayala *et al.* 2011; Meyerowitz *et al.* 2011; Iguchi *et al.* 2012). We investigated in which stress condition(s) TDP-43 was phosphorylated. Western blot analysis revealed that TDP-43 was phosphorylated at both serines 403/404 and 409/410 in the insoluble fraction after 2 h of ARS treatment (Fig. 4a), but not that after 0.5 h of ARS treatment. When serines 403/404 and 409/410 were mutated to alanines (Figure S2a), ARS-induced phosphorylation of TDP-43 was diminished (Figure S2b). Immunocytochemical analysis revealed that ARS-induced phosphorylated TDP-43 was distributed to the cytoplasm with a granular morphology, in addition being localized to the nucleus (Fig. 4c). Phosphorylated TDP-43-positive cytoplasmic compartments did not co-localize with TIA-1 (Fig. 4d), the processing body (PB) marker Dcp1a (Fig. 4d), or ubiquitin (data not shown), but co-localized with an ubiquitin-binding protein, p62 (Fig. 4e).

TDP-43 is phosphorylated by the c-jun N-terminal kinase pathway and associated with ARS-induced cytotoxicity

Previous reports have demonstrated that ARS treatment induces apoptosis cell death pathways via phosphorylation of apoptosis regulation kinases, such as c-jun N-terminal kinase (JNK), p-38 mitogen-activated protein kinase (MAPK), and extracellular signal-regulated kinase (ERK) (Namgung and Xia 2000; Ryabinina *et al.* 2006). We investigated whether these kinases are involved in the phosphorylation of TDP-43. The JNK inhibitor SP600125 and the p38 inhibitor SB203580 inhibited phosphorylation of JNK and MAPKAPK2, downstream kinase of p38, respectively, in cells treated with ARS for 2 h (Fig. 5a). In addition, the MEK inhibitor PD89059 inhibited phosphorylation of ERK both after 2 h of ARS incubation and 4.5 h after the stress was removed (Fig. 5a). All three inhibitors inhibited cleavage of caspase-3 in ARS-treated cells (Fig. 5a). Of these inhibitors, only SP600125 significantly decreased the amount of phosphorylated TDP-43 after ARS-induced stress (Fig. 5a and b), suggesting that activation of JNK is involved in the phosphorylation of TDP-43 at least in ARS-treated cells.

We next carried out a lactate dehydrogenase (LDH) release assay to investigate the effect of TDP-43 depletion on ARS-induced cytotoxicity. When non-transfected, normal HeLa cells were treated with ARS for 2 h and then recovered from this stress, cytotoxicity did not increase within the first 12 h, but then increased by as much as 5% after 15 h (data not shown), suggesting that 2 h of ARS treatment gave cells a sublethal cytotoxic injury above the recoverable, non-lethal level. When control siRNA- or TDP-43 siRNA-transfected cells were incubated in ARS-free media for 8 h after 2 h of ARS treatment, cytotoxicity was not increased in control cells. In contrast, in TDP-43-silenced cells, cytotoxicity increased by as much as 45% (Fig. 5c), suggesting that TDP-43-silenced cells could not protect themselves from ARS-induced sublethal stress, even at an early stage after the stress was removed, during which control cells remained alive.

TDP-43 depletion causes increased cytotoxicity and poly $(A)^+$ RNA destability in SH-SY5Y neuronal cells during ARS-induced oxidative stress

We also investigated whether TDP-43 depletion could cause neuronal cell death during stress. SH-SY5Y neuronal cells were more susceptible to ARS-induced oxidative stress compared with HeLa cells (data not shown). Therefore, we reduced the concentration of ARS used in the experiments from 0.5 mM to 0.25 mM. Cytotoxicity was significantly increased in TDP-43 silenced SH-SY5Y neuronal cells compared with control cells (Fig. 5d). We next carried out fluorescence *in situ* hybridization (FISH) experiments to investigate mRNA stability in stressed SH-SY5Y neuronal cells. FISH is a useful method for detecting alterations of poly $(A)^+$ RNA during ARS-induced stress (Figure S3). In the non-stressed condition, localization of poly $(A)^+$ RNA did not differ between control and TDP-43-silenced SH-SY5Y neuronal cells (Fig. 5e and f), while the poly $(A)^+$ RNA level calculated based on the fluorescence intensity per cell was slightly but significantly reduced in TDP-43-silenced cells compared with control cells (Fig. 5g). When both types of siRNA-transfected cells were incubated in ARS-free media for 3 h after 2 h of ARS treatment, the

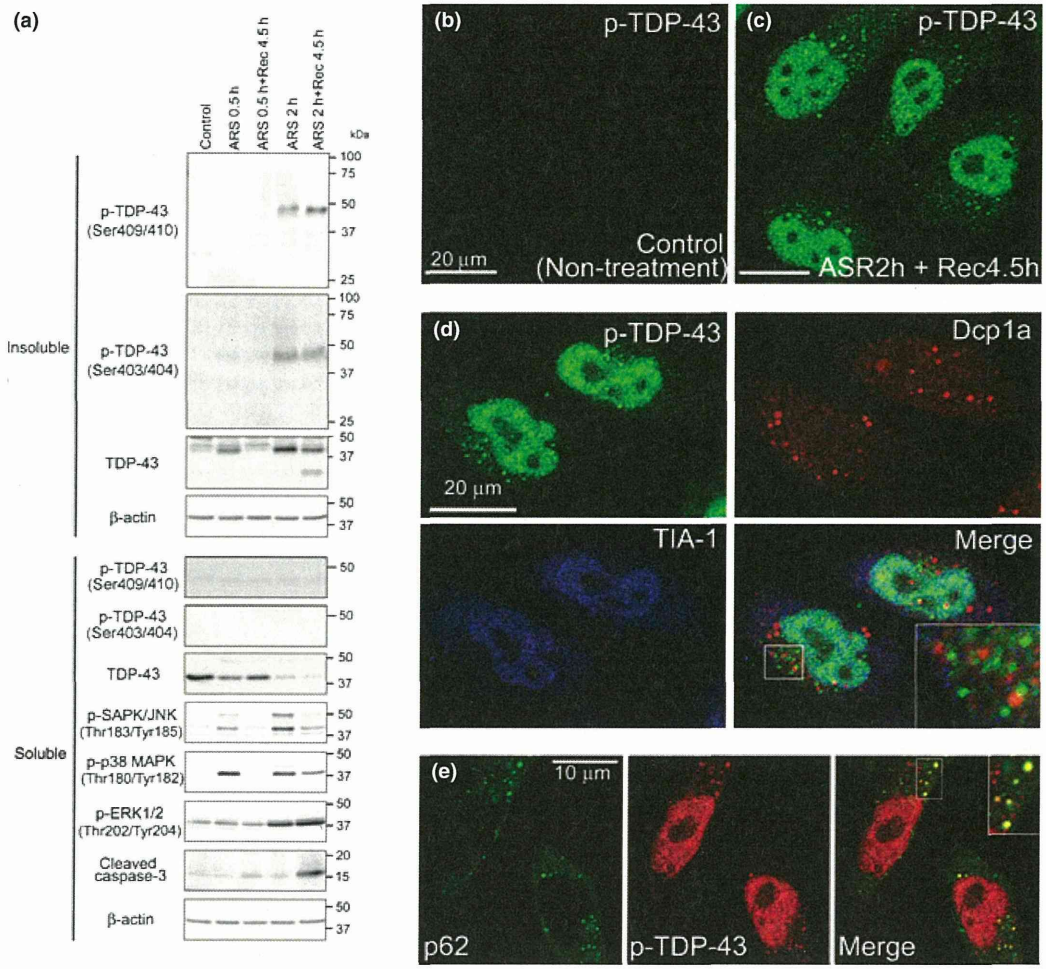

Fig. 4 (a–e) Soluble and insoluble fractions extracted from untreated HeLa cells (Control) or HeLa cells treated with 0.5 mM sodium arsenite (ARS) with or without subsequent recovery in ARS-free media, as indicated, were analyzed by immunoblotting as indicated. (b, c) Untreated HeLa cells (b) or HeLa cells treated with 0.5 mM ARS for 2 h followed by recovery in ARS-free media for 4.5 h (c) were analyzed by immunocytochemistry with anti-p-TAR DNA-binding protein 43 (p-TDP-43) (Ser409/410). The same confocal laser condition was applied to obtain both microscopic images in (b) and (c). (d, e) HeLa cells treated with 0.5 mM ARS for 2 h followed by recovery in ARS-free media for 4.5 h were analyzed by immunocytochemistry as indicated. The insets highlight that p-TDP-43 does not co-localize with Dcp1a or TIA-1 (d) but co-localizes with p62 (e).

poly $(A)^+$ RNA level in TDP-43-silenced cells was more dramatically decreased by approximately 25% compared with that in control cells (Fig. 5h–j). Thus, TDP-43 depletion reduced the poly $(A)^+$ RNA level in non-stressed, and also, more significantly, in stressed neuronal cells.

Discussion

In this study, we observed how translational control is fine-tuned in time in eukaryotic cells exposed to stress, and how TDP-43 is involved in such control. Organisms can respond to stress stimuli to adapt to changing conditions in various manners, one of which is the regulation of gene expression by post-transcriptional control (Holcik and Sonenberg 2005). As shown in this study, when cells were exposed to ARS-induced oxidative stress, actively translating polysomes were disassembled, suggesting that global translation was reduced for adaptive changes in gene expression. When the stress was short-term/non-lethal, stalled translation could be globally initiated by the removal of the stress. In contrast, exposure of cells to long-term/sublethal stress resulted in the continuous inhibition of global translational initiation, and finally led to the activation of caspase-3. Thus, we used two kinds of stress in this study, leading to non-lethal or sublethal injury, to understand the physiological roles of TDP-43 in the complex translational regulation mechanisms.

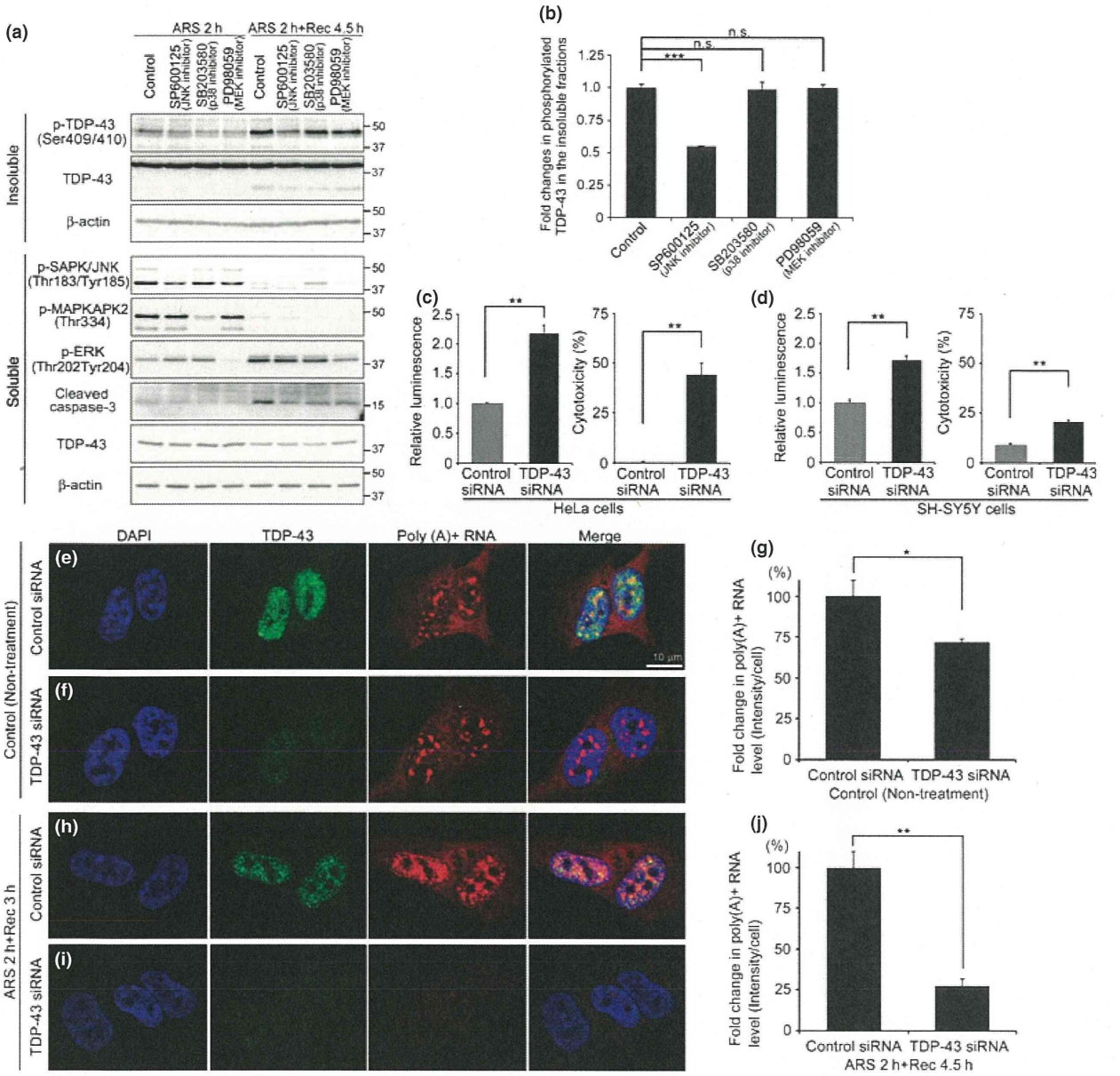

Fig. 5 (a–j) HeLa cells were pre-treated with phosphate-buffered saline (PBS) (Control), 40 μM SP600125, 5 μM SB203580, or 10 μM PD98059 for 1 h, and then treated with 0.5 mM ARS for 2 h with or without subsequent recovery in sodium arsenite (ARS)-free media for 4.5 h together with PBS or the above inhibitors as indicated. Soluble and insoluble fractions were analyzed by immunoblotting as indicated. (b) The relative levels of insoluble phosphorylated TAR DNA-binding protein 43 (TDP-43) in cells treated with 0.5 mM ARS for 2 h followed by recovery in ARS-free media for 4.5 h were quantified by densitometry and then normalized to the β-actin level. Data are presented as fold changes compared with controls (mean ± SD, $n = 4$). ***$p < 0.0001$ (one-way ANOVA with Dunnett's multiple comparison *post hoc* test). (c, d) Cytotoxicity was quantified by an lactate dehydrogenase (LDH) release assay in control siRNA and TDP-43 siRNA transfected HeLa (c) or SH-SY5Y (d) cells, which were treated with 0.5 mM (c) or 0.25 mM (d) ARS for 2 h followed by recovery in ARS-free media for 8 h, as described in the supplemental methods section (mean ± SD, $n = 3$). **$p < 0.01$ (paired Student's *t*-test). (e–j) Control siRNA (e, h) or TDP-43 siRNA (f, i) transfected SH-SY5Y cells were untreated (e, f) or treated with 0.25 mM ARS with subsequent recovery in ARS-free media for 3 h (h, i), and then analyzed by fluorescence *in situ* hybridization (red) with immunocytochemistry with anti-TDP-43 antibody (green), as indicated. The same confocal laser condition was applied to obtain all microscopic images in (e, f, h, i). The poly $(A)^+$ RNA level in each cell was calculated by measuring the fluorescent intensity per cell (g, j) as described in the Supplementary methods (mean ± SD, $n = 3$). *$p < 0.05$, **$p < 0.01$ (paired Student's *t*-test).

Although TDP-43 did not associate with actively translating polysomes under the non-stress, steady-state condition, ARS-induced stress stimuli led to the association of TDP-43 with stalled ribosomes by binding to mRNA (Fig. 1b). This association with ribosomes was temporary and reversible when the stress was non-lethal because it was immediately dissolved when the stress was removed (Fig. 1c–e). In addition, the alteration of the solubility of component proteins in SGs including TDP-43 was also temporary and reversible under the non-lethal stress condition (Fig. 3b), suggesting that SGs are not rigid, inflexible insoluble aggregates, which might enable cells to dynamically regulate gene expression to adapt to a new condition. In contrast, when cells were subjected to sublethal stress, TDP-43 was excluded from SGs (Fig. 2i) and shifted to the heavier fractions than the monosomal peak (Fig. 1f). Notably, eIF3 was also shifted to the heavy fraction. However, given that the shift of TDP-43 to the heavy fractions was independent of mRNA binding (Fig. 1m), this shift might represent aggregation of TDP-43. In addition, the sublethal stress caused SARK-insoluble TDP-43 aggregation that was retained after the stress was removed (Fig. 3b and e). Thus, TDP-43 can shuttle in (Fig. 2g) and out (Fig. 2i) of SGs in response to a change in stress conditions. Previous FRAP analysis revealed that a number of SG-associated RNA-binding proteins rapidly shuttle in and out of SGs; therefore, internal compositions in RNA granules may be modified according to the stress condition (Kedersha *et al.* 2000, 2005). Although the C-terminal region of TDP-43 includes a PrP-like domain that gives it a tendency to undergo self-assembly (Udan and Baloh 2011), our analysis revealed that RRM domains were responsible for ARS-induced increased insolubility (Fig. 3g). Therefore, nucleic acid binding appears to contribute to the initiation of TDP-43 aggregation. This result is consistent with the recent concept that RNA molecules play important roles in prion protein aggregation, resulting in cellular toxicity (Gomes *et al.* 2008). In contrast, the C-terminus itself has a tendency to become insoluble regardless of the stress condition. In addition to self-assembly, the PrP-like domain has another property: infectious propagation. Therefore, the C-terminal PrP-like domain in TDP-43 might contribute to transmissible aggregation.

TDP-43 was phosphorylated by the JNK pathway following ARS-induced activation (Fig. 5b), as previously described (Meyerowitz *et al.* 2011). Notably, TDP-43 was phosphorylated several hours after phosphorylation of JNK occurred. This delay indicates that TDP-43 would not be phosphorylated directly by JNK, and rather TDP-43 phosphorylation might be located downstream of JNK-associated pathway. A previous study showed that JNK pathways contributed to ARS-induced apoptotic cell death (Namgung and Xia 2000). Therefore, we investigated whether TDP-43 was involved in ARS-induced apoptosis. In TDP-43-silenced cells, cytotoxicity was significantly increased after sublethal stress (Fig. 5c and d). The cytotoxicity seen in TDP-43-silenced cells occurred at an early stage when cytotoxicity was not induced in control cells, suggesting that TDP-43 is required for the initial cell survival system(s) that enable cells to protect themselves from sublethal injury. This might support the recent concept that TDP-43 dysfunction or loss of function is responsible for the cellular toxicity in ALS and FTLD (Xu 2012). Moreover, TDP-43 silencing caused a decrease in the amount of non-translating, stalled mRNA, monitored based on absorbance at 260 nm (Fig. 2l), and poly $(A)^+$ RNA (Fig. 5j) in cells exposed to sublethal stress. A previous report showed that tristetrapolin, a SG-associated protein, was excluded from SGs under conditions of ARS-induced stress, leading to inhibition of the degradation of AU-rich element (ARE)-containing mRNAs (Stoecklin *et al.* 2004). Shuttling of TDP-43 in and out of SGs might be also essential for mRNA stability.

In conclusion, TDP-43 can shuttle in and out of SGs according to the level of stress. Under the sublethal stress condition, the biochemical alterations of TDP-43 reminiscent of the pathogenic changes were observed, and TDP-43 contributed to mRNA stability and cell survival. SGs are thought to contain components which are linked to apoptosis (Kim *et al.* 2005; Arimoto *et al.* 2008). Further investigation of the pathological roles of TDP-43 in apoptosis regulation would provide important insights into the pathogenesis of these diseases and potential new therapeutic strategies.

Acknowledgement

This study was supported in part by the Kurata Memorial Hitachi Science and Technology Foundation (to S.H.); Grants-in-Aid for Young Scientist 23791008 (to S.H.), Grants-in-Aid for Scientific Research (to K.W.) and "Integrated research on neuropsychiatric disorders" carried out under the Strategic Research Program for Brain Sciences (to Y.N.) from the Ministry of Education, Culture, Sports, Science; Grants-in-Aid for Scientific Research from the Ministry of Health, Labour and Welfare 10102894 and 10103470 (to H.A.) of Japan (to K.W.); the Ministry of Education, Culture, Science 09019658 (to H.A.) and Technology of Japan, and a grant from Japan Science and Technology Agency (to K.W.).

Conflict of interest

None declared.

Supporting information

Additional supporting information may be found in the online version of this article at the publisher's web-site.

Figure S1. (a–d) Cell extracts obtained from HeLa cells treated with 0.5 mM ARS for 1 h (a).

Figure S2. (a) The domain architectures of wild-type (WT) TDP-43 or TDP-43 bearing mutation of serines (Ser403/404/409/410) to alanines (Ala) are shown schematically.